Available online at www.sciencedirect.com
ScienceDirect
Journal of Sound and Vibration 302 (2007) 185–196
JOURNAL OF SOUND AND VIBRATION
www.elsevier.com/locate/jsvi

Free vibration analysis of cylindrical helical springs by the pseudospectral method

Jinhee Lee*

Department of Mechano-Informatics, Hongik University, Chochiwon, Yeonki-gun, Choongnam 339-701, Republic of Korea

Received 14 March 2006; received in revised form 17 November 2006; accepted 19 November 2006
Available online 11 January 2007

Abstract

The pseudospectral method is applied to the free vibration analysis of cylindrical helical springs. The displacements and the rotations are approximated by the series expansions of Chebyshev polynomials and the governing equations are collocated. The number of collocation points is chosen to be less than the number of the expansion terms to handle the boundary condition. Numerical examples are provided for fixed–fixed, free–free, fixed–free and hinged–hinged boundary conditions. The results show good agreement with those of the transfer matrix method and the dynamic stiffness method. The formulation of the pseudospectral method is straightforward and shows an exponential rate of convergence with mesh refinement.

1. Introduction

Helical springs are widely used in many engineering applications. Because of their importance the free vibration analysis of helical springs has been extensively investigated and new methods have been proposed since Wittrick [1] derived a set of 12 linear coupled partial differential equations for a uniform helical spring based on the Timoshenko beam theory.

The transfer matrix method is one of the most favored tools in the free vibration analysis of helical springs. Pearson [2] extended Wittrick's equations to include the effects of static loading and obtained numerical solutions for buckling and free vibrations by the transfer matrix method. Nagaya et al. [3] obtained the transfer matrix by combining the point transfer matrix and the field transfer matrix which was derived from the solution of the fundamental equation of the curved beam theory. Yildirim [4] used the Cayley–Hamilton theorem to solve the free vibration problem of helical springs by the transfer matrix method. Yildirim [5,6] also conducted series of studies to compute the eigenvalues of helical springs of arbitrary shape. Becker et al. [7] investigated the effect of static axial compression upon the natural frequencies of helical springs by the transfer matrix method. Lee and Thompson [8] used the dynamic stiffness method to calculate the natural frequencies of helical springs and compared the results with those of the transfer matrix and the finite element method.

*Tel.: +82 41 860 2589; fax: +82 41 862 2664.
E-mail address: jinhlee@wow.hongik.ac.kr.

0022-460X/$ - see front matter © 2006 Elsevier Ltd. All rights reserved.
doi:10.1016/j.jsv.2006.11.008

Another approach is the finite element method. Mottershead [9] developed finite elements for the solution of the eigenvalue problem of helical springs. Xiong and Tabarrok [10] developed a finite element formulation for the vibration analysis of spatially curved and twisted rods which took account the initial moments and shear forces as well as initial deformations. Stander and Du Preez [11] investigated the reduced integration rules for the finite element analysis of helical springs. In the present work, the pseudospectral method is applied to the free vibration analysis of cylindrical helical springs.

2. The pseudospectral method

In the spectral methods it is assumed that $u(x)$, the solution to the differential equation with homogeneous boundary condition, can be approximated by a sum of K basis functions $\phi_k(x)$

$$u(x) \approx u_K(x) = \sum_{k=1}^{K} a_k \phi_k(x). \tag{1}$$

When this series is substituted into the differential equation

$$Lu = f(x), \tag{2}$$

where L is the operator of the equation, the residual function is defined by

$$\Re(x; a_1, a_2, \ldots, a_K) = Lu_K - f. \tag{3}$$

If the basis functions $\phi_k(x)$ individually satisfy the homogeneous boundary condition on $u(x)$, so does their sum. Since the residual function is identically 0 for the exact solution, it is important to find the series coefficients a_k in such a way that the residual function is made as small as possible. The pseudospectral and different spectral methods differ mainly in their way of minimizing $\Re(x; a_1, a_2, \ldots, a_k)$.

The pseudospectral method associates a grid of collocation points with each basis set. In the pseudospectral method the coefficients a_k are found by requiring the residual function to vanish at the collocation points

$$\Re(x_i; a_1, a_2, \ldots, a_K) = 0 \quad i = 1, 2, \ldots, K. \tag{4}$$

As the residual function is forced to vanish at the collocation points, it will be smaller and smaller in the gaps between the collocation points so that $u_k(x)$ will converge to $u(x)$ as K increases. Various methods such as the basis recombination and the boundary bordering technique have been devised to deal with the nonhomogeneous boundary conditions.

Chebyshev polynomials, Legendre polynomials and Fourier series are the typical basis functions of the pseudospectral method. Since the basis functions can be differentiated analytically and since each spectral coefficient a_k is determined by all the grid point values of $u(x)$, the pseudospectral method is considered to possess high accuracy and exponential rate of convergence with grid refinement on smooth and regular domains. The major drawbacks of the pseudospectral method are that it suffers heavier losses of accuracy and efficiency on irregular domains than the lower-order algorithms and that it is more costly per degree of freedom (dof) than the discretization methods because the pseudospectral method generates algebraic equations with full matrices.

As the formulation is straightforward and powerful enough to produce approximate solutions close to exact solutions, the pseudospectral method has been successfully applied to the problems of computational physics and fluid mechanics [12]. Lee and Schultz applied the pseudospectral method to the eigenvalue problems of Timoshenko beams and axisymmetric Mindlin plates [13]. Lee used the pseudospectral method to investigate the free vibration of double-span Timoshenko beams, where basis functions are assumed for each section separately and the continuity conditions at the intermediate support and the boundary conditions are considered as the side constraints so that the number of dofs matches the number of the pseudospectral expansion coefficients [14].

3. Pseudospectral formulations for a helical spring

Fig. 1 describes the geometry of a typical helical spring. R, s and α are the centerline radius of the helix, the distance along the helical spring and the pitch angle of the helix, respectively.

Assuming the centroid of the cross-section and the shear centerline to coincide and neglecting the warping of the cross-section due to torsion, Yildirim [4,5] derived the equations of motion of a uniform cylindrical helical spring for the free vibration as

$$\frac{dT_t}{ds} - \chi T_n = -\omega^2 \rho A U_t, \tag{5a}$$

$$\frac{dT_n}{ds} + \chi T_t - \tau T_b = -\omega^2 \rho A U_n, \tag{5b}$$

$$\frac{dT_b}{ds} + \tau T_n = -\omega^2 \rho A U_b, \tag{5c}$$

$$\frac{dM_t}{ds} - \chi M_n = -\omega^2 \rho J \Omega_t, \tag{5d}$$

$$\frac{dM_n}{ds} - T_b + \chi M_t - \tau M_b = -\omega^2 \rho I_n \Omega_n, \tag{5e}$$

$$\frac{dM_b}{ds} + T_n + \tau M_n = -\omega^2 \rho I_b \Omega_b \tag{5f}$$

for harmonic motion at natural frequency ω in radian/second. U_t, U_n and U_b represent the displacements, and Ω_t, Ω_n and Ω_b are the rotations. Subscripts t, n and b stand for the tangential direction, the normal direction and the binormal direction, respectively. A, I_n, I_b and J are the cross sectional area, the second moments of area with respect to the normal axis and to the binormal axis, and the torsional moment of inertia of the cross

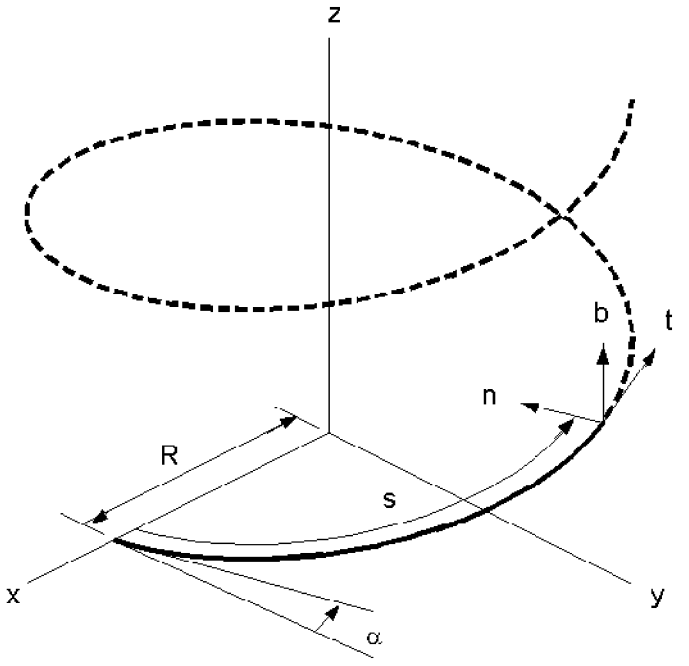

Fig. 1. The geometry of a typical helical spring.

section. $\chi = \cos^2\alpha/R$, $\tau = \cos\alpha \sin\alpha/R$ and ρ are the curvature, the tortuosity of the helix and the density, respectively.

T_t, T_n and T_b are the components of the internal forces in the t, n and b directions, and M_t, M_n and M_b are the components of the internal moments in the t, n and b directions, respectively, which are defined as [4,5]

$$T_t = EA\left(\frac{\mathrm{d}U_t}{\mathrm{d}s} - \chi U_n\right), \tag{6a}$$

$$T_n = \frac{GA}{\beta_n}\left(\frac{\mathrm{d}U_n}{\mathrm{d}s} + \chi U_t - \tau U_b - \Omega_b\right), \tag{6b}$$

$$T_b = \frac{GA}{\beta_b}\left(\frac{\mathrm{d}U_b}{\mathrm{d}s} + \tau U_n + \Omega_n\right), \tag{6c}$$

$$M_t = GJ\left(\frac{\mathrm{d}\Omega_t}{\mathrm{d}s} - \chi\Omega_n\right), \tag{6d}$$

$$M_n = EI_n\left(\frac{\mathrm{d}\Omega_n}{\mathrm{d}s} + \chi\Omega_t - \tau\Omega_b\right), \tag{6e}$$

$$M_b = EI_b\left(\frac{\mathrm{d}\Omega_b}{\mathrm{d}s} + \tau\Omega_n\right). \tag{6f}$$

Fig. 2 shows the components of internal forces and moments. E and G are Young's modulus and the shear modulus. β_n and β_b are the Timoshenko coefficients. The substitution of (6a)–(6f) into (5a)–(5f) yields the following set of governing equations:

$$EA\frac{\mathrm{d}^2U_t}{\mathrm{d}s^2} - \chi^2\frac{GA}{\beta_n}U_t - \chi\left(EA + \frac{GA}{\beta_n}\right)\frac{\mathrm{d}U_n}{\mathrm{d}s} + \chi\tau\frac{GA}{\beta_n}U_b + \chi\frac{GA}{\beta_n}\Omega_b = -\omega^2\rho A U_t, \tag{7a}$$

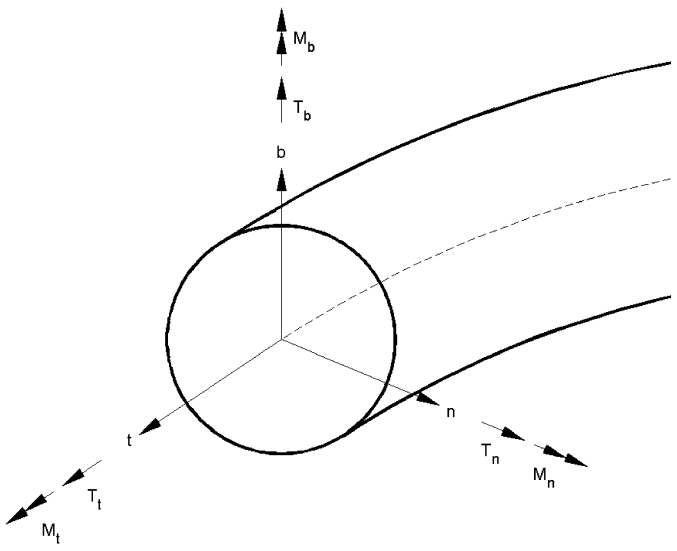

Fig. 2. The components of internal forces and moments.

$$\chi\left(EA+\frac{GA}{\beta_n}\right)\frac{\mathrm{d}U_t}{\mathrm{d}s}+\frac{GA}{\beta_n}\frac{\mathrm{d}^2U_n}{\mathrm{d}s^2}-\left(\chi^2EA+\tau^2\frac{GA}{\beta_b}\right)U_n - \tau\left(\frac{GA}{\beta_n}+\frac{GA}{\beta_b}\right)\frac{\mathrm{d}U_b}{\mathrm{d}s}-\tau\frac{GA}{\beta_b}\Omega_n-\frac{GA}{\beta_n}\frac{\mathrm{d}\Omega_b}{\mathrm{d}s}=-\omega^2\rho AU_n, \tag{7b}$$

$$\chi\tau\frac{GA}{\beta_n}U_t+\tau\left(\frac{GA}{\beta_n}+\frac{GA}{\beta_b}\right)\frac{\mathrm{d}U_n}{\mathrm{d}s}+\frac{GA}{\beta_b}\frac{\mathrm{d}^2U_b}{\mathrm{d}s^2}-\tau^2\frac{GA}{\beta_n}U_b+\frac{GA}{\beta_b}\frac{d\Omega_n}{\mathrm{d}s}-\tau\frac{GA}{\beta_n}\Omega_b=-\omega^2\rho AU_b, \tag{7c}$$

$$GJ\frac{\mathrm{d}^2\Omega_t}{\mathrm{d}s^2}-\chi^2EI_n\Omega_t-\chi(EI_n+GJ)\frac{\mathrm{d}\Omega_n}{\mathrm{d}s}+\chi\tau EI_n\Omega_b=-\omega^2\rho J\Omega_t, \tag{7d}$$

$$-\tau\frac{GA}{\beta_b}U_n-\frac{GA}{\beta_b}\frac{\mathrm{d}U_b}{\mathrm{d}s}+\chi(EI_n+GJ)\frac{\mathrm{d}\Omega_t}{\mathrm{d}s}+EI_n\frac{\mathrm{d}^2\Omega_n}{\mathrm{d}s^2} -\left(\frac{GA}{\beta_b}+\chi^2GJ+\tau^2EI_b\right)\Omega_n-\tau(EI_n+EI_b)\frac{\mathrm{d}\Omega_b}{\mathrm{d}s}=-\omega^2\rho I_n\Omega_n, \tag{7e}$$

$$\chi\frac{GA}{\beta_n}U_t+\frac{GA}{\beta_n}\frac{\mathrm{d}U_n}{\mathrm{d}s}-\tau\frac{GA}{\beta_n}U_b+\chi\tau EI_n\Omega_t+\tau(EI_n+EI_b)\frac{\mathrm{d}\Omega_n}{\mathrm{d}s} +EI_b\frac{\mathrm{d}^2\Omega_b}{\mathrm{d}s^2}-\left(\frac{GA}{\beta_n}+\tau^2EI_n\right)\Omega_b=-\omega^2\rho I_b\Omega_b. \tag{7f}$$

Typical boundary conditions are represented by

$$\textit{Fixed}: \quad U_t=0, \quad U_n=0, \quad U_b=0, \quad \Omega_t=0, \quad \Omega_n=0, \quad \Omega_b=0, \tag{8a}$$

$$\textit{Hinged}: \quad U_t=0, \quad U_n=0, \quad U_b=0, \quad M_t=0, \quad M_n=0, \quad M_b=0, \tag{8b}$$

$$\textit{Free}: \quad T_t=0, \quad T_n=0, \quad T_b=0, \quad M_t=0, \quad M_n=0, \quad M_b=0. \tag{8c}$$

When the range of the independent variable is given by $(0\leqslant s\leqslant S)$, where $S=2\pi nR\sqrt{1+\tan^2\alpha}$ is the total length of the spring and n is the number of turns of the helix, it is convenient to use the normalized variable

$$\xi=\frac{2s-S}{S}\in[-1,1]. \tag{9}$$

The displacements and rotations are expressed as sums of Chebyshev polynomials. Lee and Schultz suggested an efficient way to handle the boundary conditions by adopting a larger number of expansion terms than that of the collocation points [13]. U_t, U_n, U_b, Ω_t, Ω_n and Ω_b are approximated as series expansions as follows:

$$\begin{aligned}
U_t(\xi)&=\sum_{k=1}^{K+2}a_kT_{k-1}(\xi),\\
U_n(\xi)&=\sum_{k=1}^{K+2}b_kT_{k-1}(\xi),\\
U_b(\xi)&=\sum_{k=1}^{K+2}c_kT_{k-1}(\xi),\\
\Omega_t(\xi)&=\sum_{k=1}^{K+2}d_kT_{k-1}(\xi),\\
\Omega_n(\xi)&=\sum_{k=1}^{K+2}e_kT_{k-1}(\xi),\\
\Omega_b(\xi)&=\sum_{k=1}^{K+2}f_kT_{k-1}(\xi),
\end{aligned} \tag{10}$$

where a_k, b_k, c_n, d_k, e_k and f_k are the expansion coefficients. K and T_{k-1} are the number of collocation points and the Chebyshev polynomial of the first kind of degree of $k-1$, respectively.

Expansions (10) are substituted into Eqs. (7a–f), and are collocated at the Gauss-Lobatto collocation points

$$\xi_i = -\cos\frac{\pi(2i-1)}{2K} \quad (i = 1, 2, \ldots, K) \tag{11}$$

to yield the collocated governing equations as given in Appendix A.

The collocated governing equations (A1)–(A6) can be rearranged in the matrix form

$$[H]\{\delta\} + [H^*]\{\delta^*\} = \omega^2\big([F]\{\delta\} + [F^*]\{\delta^*\}\big), \tag{12}$$

where the vectors in Eq. (12) are defined as

$$\begin{aligned}\{\delta\} &= \{a_1 a_2 \cdots a_K b_1 b_2 \cdots b_K c_1 c_2 \cdots c_K d_1 d_2 \cdots d_K e_1 e_2 \cdots e_K f_1 f_2 \cdots f_K\}^{\mathrm{T}},\\ \{\delta^*\} &= \{a_{K+1} a_{K+2} b_{K+1} b_{K+2} c_{K+1} c_{K+2} d_{K+1} d_{K+2} e_{K+1} e_{K+2} f_{K+1} f_{K+2}\}^{\mathrm{T}}.\end{aligned} \tag{13}$$

$[H]$ and $[F]$ are matrices of order $6K$, and the size of matrices $[H^*]$ and $[F^*]$ is $6K \times 12$. The total number of equations in (12) is $6K$ whereas the total number of unknowns is $6(K+2)$. The remaining twelve equations are obtained from the boundary condition. The boundary conditions (8a–c) at $\xi_b = \pm 1$ are expressed by the series expansions (10) and are given in Appendix B.

The formation of the boundary condition set can be accomplished by picking one set of condition up from Eqs. (B1)–(B3) at $\xi_b = -1$ and another at $\xi_b = 1$. The fixed–fixed boundary condition set, for example, consists of the following 12 equations:

$$\begin{aligned}&\sum_{k=1}^{K+2} a_k T_{k-1}(-1) = 0, \quad \sum_{k=1}^{K+2} b_k T_{k-1}(-1) = 0, \quad \sum_{k=1}^{K+2} c_k T_{k-1}(-1) = 0,\\ &\sum_{k=1}^{K+2} d_k T_{k-1}(-1) = 0, \quad \sum_{k=1}^{K+2} e_k T_{k-1}(-1) = 0, \quad \sum_{k=1}^{K+2} f_k T_{k-1}(-1) = 0,\\ &\sum_{k=1}^{K+2} a_k T_{k-1}(1) = 0, \quad \sum_{k=1}^{K+2} b_k T_{k-1}(1) = 0, \quad \sum_{k=1}^{K+2} c_k T_{k-1}(1) = 0,\\ &\sum_{k=1}^{K+2} d_k T_{k-1}(1) = 0, \quad \sum_{k=1}^{K+2} e_k T_{k-1}(1) = 0, \quad \sum_{k=1}^{K+2} f_k T_{k-1}(1) = 0.\end{aligned} \tag{14}$$

The boundary condition set can be rearranged in the matrix form

$$[U]\{\delta\} + [V]\{\delta^*\} = \{0\}, \tag{15}$$

where $\{0\}$ is a zero vector. The size of matrix $[U]$ is $12 \times 6K$, and $[V]$ is a matrix of order 12. Since $\{\delta^*\}$ in Eq. (15) can be expressed as

$$\{\delta^*\} = -[V]^{-1}[U]\{\delta\}, \tag{16}$$

Eq. (12) can be reformulated as

$$\big([H] - [H^*][V]^{-1}[U]\big)\{\delta\} = \omega^2\big([F] - [F^*][V]^{-1}[U]\big)\{\delta\}. \tag{17}$$

The solution of Eq. (17) yields the estimates for ω and $\{\delta\}$. Once $\{\delta\}$ is obtained the corresponding mode shapes are computed by Eqs. (10) and (16). This procedure can be applied to any boundary condition set of fixed–fixed, hinged–hinged, free–free, fixed–hinged, fixed–free, or hinged–free boundary condition.

4. Numerical examples and discussions

A convergence check of the natural frequencies of a helical spring for fixed–fixed boundary condition is carried out and the results are given in Table 1. The spring has a wire radius of 0.5 mm, a centerline radius of 5 mm and a height of 36 mm. The spring has 7.6 turns giving a helix pitch angle of 8.5744°.

Table 1
Convergence test of the natural frequencies in Hz of a cylindrical helical spring

Mode	Present study					Transfer matrix method [4]	Transfer matrix method [7]	Finite element method [9]
	$K=10$	$K=20$	$K=30$	$K=40$	$K=50$			
1	467.7	463.9	443.3	393.5	393.5	393.5	393.5	396.0
2	536.2	527.6	460.7	396.1	396.1	395.9	396.1	397.0
3	917.4	907.3	481.4	462.9	462.9	462.8	462.8	469.0
4	1054.7	1032.8	530.3	525.7	525.7	525.5	525.7	532.0
5	1332.0	1315.8	904.7	863.8	863.8	864.0	863.8	887.0
6	1532.6	1499.2	935.5	877.0	877.0	876.8	876.9	900.0
7	1691.1	1591.9	1009.1	913.8	913.8	914.3	913.7	937.0
8	1961.5	1714.6	1046.8	1037.5	1037.5	1037.0	1037.5	1067.0
9	2008.8	1786.3	1323.9	1310.7	1310.7	1310.5	1310.6	1348.0
10	2285.1	1920.5	1452.4	1364.6	1364.6	1363.8	1364.6	1409.0

Fixed–fixed boundary condition, wire radius $r=0.5\,\text{mm}$, $R=5\,\text{mm}$, $\alpha=8.5744$, $n=7.6$, $\beta_n=1.1$, $\beta_b=1.1$, $\rho=7900\,\text{kg/m}^3$, $E=2.06\times10^{11}\,\text{N/m}^2$, Poisson's ratio $v=0.3$.

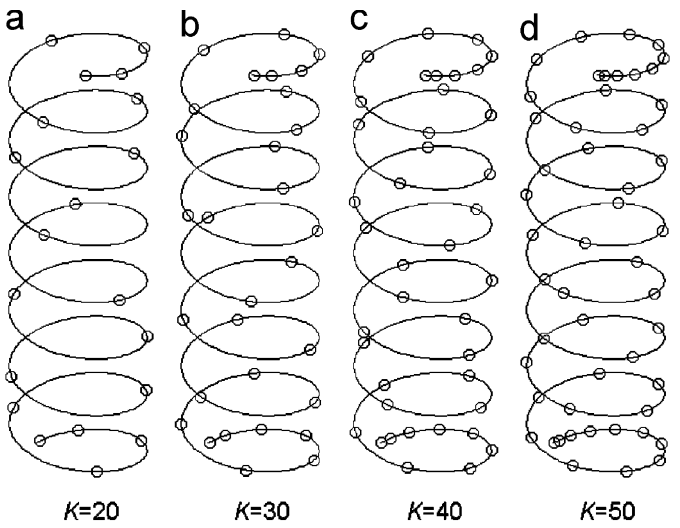

Fig. 3. The distribution of the collocation points along a cylindrical helical spring for different numbers of collocation points K ($R=5\,\text{mm}$, $\alpha=8.5744^\circ$, $n=7.6$).

The number of collocation points which determines the accuracy of the solution ranges from $K=10$ to $K=50$ in the convergence check. Fig. 3 shows how the collocation points are distributed along the helical spring for $K=20$, 30, 40, and 50. Table 1 shows the rapid convergence nature of the pseudospectral method that requires less than 40 collocation points for the ten lowest natural frequencies to converge to four significant figures. The converged frequencies are in fair agreement with those of Yildirim [4], Becker et al. [7] and Mottershead [9]. Fig. 4 shows how the mode shapes of mode 1, mode 3, and mode 5 change as K increases. It confirms that the mode shapes for $K=40$ are identical to those for $K=50$, which indicates that the convergence is achieved. Fig. 4 shows that mode 1, mode 3 and mode 5 are predominantly longitudinal for $K=20$. When the solution is converged mode 1 and mode 5 are predominantly transverse, and mode 3 is predominantly longitudinal, respectively.

The natural frequencies computed by the pseudospectral method with $K=50$ for fixed–fixed, free–free, fixed–free and hinged–hinged boundary conditions are given in Table 2, where the natural frequencies computed by the dynamic stiffness method [8] are given for comparison. The helical spring in this example has a wire radius of 6 mm, a centerline radius of 65 mm and a height of 320 mm. The spring has 6 turns giving a

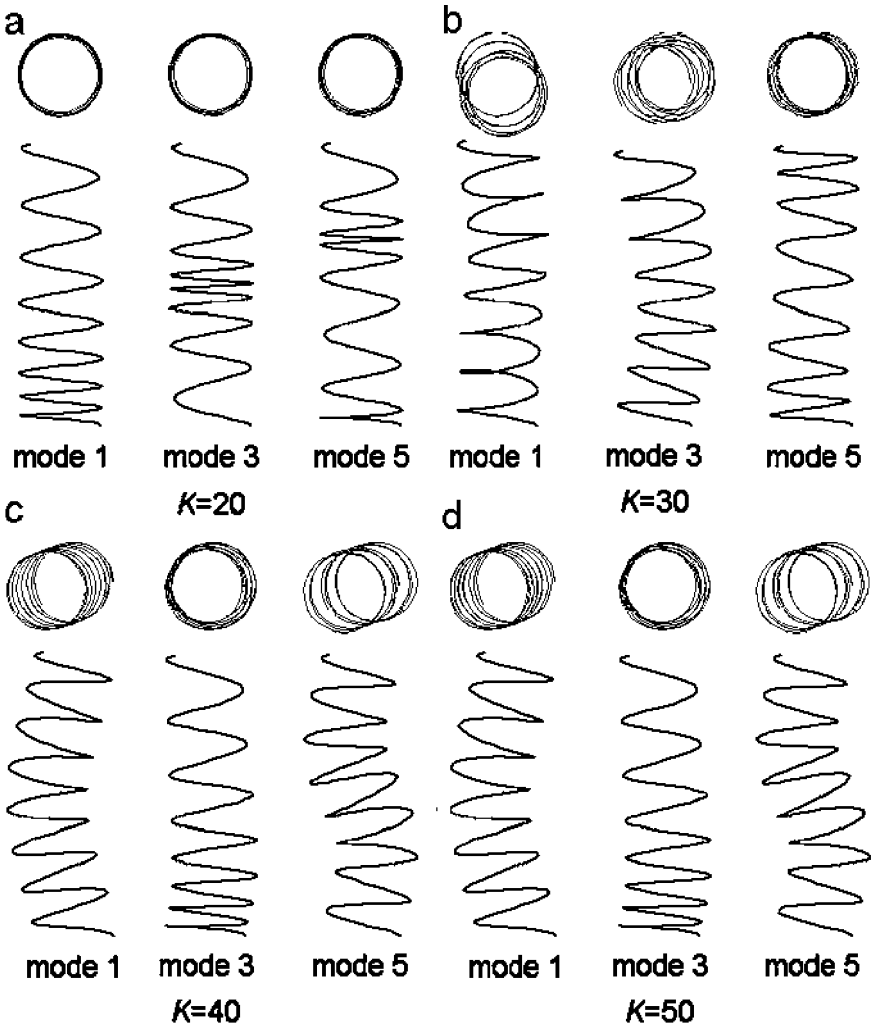

Fig. 4. Mode shapes of a cylindrical helical spring for different numbers of collocation points K (top view and plan view, fixed–fixed boundary condition, wire radius $r = 0.5\,\text{mm}$, $R = 5\,\text{mm}$, $\alpha = 8.5744^\circ$, $n = 7.6$, $\beta_n = 1.1$, $\beta_b = 1.1$, $\rho = 7900\,\text{kg/m}^3$, $E = 2.06 \times 10^{11}\,\text{N/m}^2$, Poisson's ratio $v = 0.3$).

helix pitch angle of 7.44°. The results of Table 2 show that they are in excellent agreement with those of the dynamic stiffness method [8] for various boundary conditions. The easy implementation of the boundary condition is one of the merits of the pseudospectral method. Any set of boundary condition can be merged into the governing equations systematically by the procedure explained in Eqs. (14)–(17).

The number of collocation points K that is required for the convergence of the solution is of great concern. The effects of the boundary condition, the number of turns of the helix and the centerline radius of the helix on the convergence are investigated, and the results are given in Tables 3–5. Tables 3–5 show that larger number of K is required for the convergence of the solution as the number of turns of the helix increases, while the influence of the boundary condition and the helix radius is limited.

5. Conclusions

The pseudospectral method is applied to the free vibration analysis of cylindrical helical springs and numerical examples are provided for fixed–fixed, free–free, fixed–free and hinged–hinged boundary conditions. The displacements and the rotations of the spring are approximated by the series expansions of

Table 2
Natural frequencies in Hz of a cylindrical helical spring

Boundary condition	1	2	3	4	5	6	7	8
Fixed–fixed								
Present study	40.993	45.134	46.950	47.725	81.089	88.974	91.585	93.171
Dynamic stiffness [8]	40.994	45.135	46.951	47.726	81.091	88.976	91.586	93.173
Free–free								
Present study	41.961	43.309	44.106	49.384	81.176	86.720	88.302	94.926
Dynamic stiffness [8]	41.962	43.309	44.106	49.384	81.178	86.721	88.303	94.927
Fixed–free								
Present study	9.4718	9.4997	21.358	24.170	42.100	42.857	63.107	71.205
Dynamic stiffness [8]	9.4719	9.4998	21.359	24.170	42.101	42.857	63.109	71.205
Hinged–hinged								
Present study	28.516	29.171	31.161	33.784	70.124	74.721	78.098	79.629
Dynamic stiffness [8]	28.516	29.171	31.162	33.784	70.125	74.721	78.099	79.630

Wire radius $r = 6\,\text{mm}$, $R = 65\,\text{mm}$, $\alpha = 7.44^\circ$, $n = 6$, $\beta_n = 1.1$, $\beta_b = 1.1$, $\rho = 7800\,\text{kg/m}^3$, $E = 2.09 \times 10^{11}\,\text{N/m}^2$, Poisson's ratio $v = 0.28$, $K = 50$.

Table 3
Number of collocation points K required for the convergence of lowest eight natural frequencies to five figures for different boundary conditions

Boundary condition	Fixed–fixed	Free–free	Fixed–free	Hinged–hinged
K	34	31	32	32

Wire radius $r = 6\,\text{mm}$, $R = 65\,\text{mm}$, $\alpha = 7.44^\circ$, $n = 6$, $\beta_n = 1.1$, $\beta_b = 1.1$, $\rho = 7800\,\text{kg/m}^3$, $E = 2.09 \times 10^{11}\,\text{N/m}^2$, Poisson's ratio $v = 0.28$.

Table 4
Number of collocation points K required for the convergence of lowest eight natural frequencies to five figures for different numbers of turns of the helix n

n	3	6	12
K	20	34	53

Fixed–fixed boundary condition, wire radius $r = 6\,\text{mm}$, $R = 65\,\text{mm}$, $\alpha = 7.44^\circ$, $\beta_n = 1.1$, $\beta_b = 1.1$, $\rho = 7800\,\text{kg/m}^3$, $E = 2.09 \times 10^{11}\,\text{N/m}^2$, Poisson's ratio $v = 0.28$.

Table 5
Number of collocation points K required for the convergence of lowest eight natural frequencies to five figures for different radii of helix R

R	32.5 mm	65 mm	130 mm
K	34	34	32

Fixed–fixed boundary condition, wire radius $r = 6\,\text{mm}$, $\alpha = 7.44^\circ$, $n = 6$, $\beta_n = 1.1$, $\beta_b = 1.1$, $\rho = 7800\,\text{kg/m}^3$, $E = 2.09 \times 10^{11}\,\text{N/m}^2$, Poisson's ratio $v = 0.28$.

Chebyshev polynomials. To handle the boundary condition the number of collocation points is chosen to be less than the number of the expansion terms. The boundary condition is considered as the side constraints, and the set of algebraic equations is condensed so that the number of dofs of the problem matches the total number of the expansion coefficients. The example problems demonstrate the rapid convergence nature of the

pseudospectral method. The parameters that affect the convergence of the solution of the pseudospectral method are investigated. It is found that the number of turns of the helix plays an important role on the convergence of the solution. The formulation of the pseudospectral method is straightforward and efficient for writing a code for computation. The results of present study show good agreement with those of the transfer matrix method and the dynamic stiffness method. The pseudospectral method will be applied to various problems such as the forced vibration analysis and multidimensional problems in the future.

Appendix A. Collocated governing equations

$$\sum_{k=1}^{K+2} a_k \left\{ \frac{4EA}{S^2} T''_{k-1}(\xi_i) - \chi^2 \frac{GA}{\beta_n} T_{k-1}(\xi_i) \right\} - \sum_{k=1}^{K+2} b_k \frac{2\chi}{S} \left(EA + \frac{GA}{\beta_n} \right) T'_{k-1}(\xi_i) + \sum_{k=1}^{K+2} c_k \chi\tau \frac{GA}{\beta_n} T_{k-1}(\xi_i) + \sum_{k=1}^{K+2} f_k \chi \frac{GA}{\beta_n} T_{k-1}(\xi_i) = -\omega^2 \rho A \sum_{k=1}^{K+2} a_k T_{k-1}(\xi_i), \tag{A.1}$$

$$\sum_{k=1}^{K+2} a_k \frac{2\chi}{S} \left(EA + \frac{GA}{\beta_n} \right) T'_{k-1}(\xi_i) + \sum_{k=1}^{K+2} b_k \left\{ \frac{4}{S^2} \frac{GA}{\beta_n} T''_{k-1}(\xi_i) - \left(\chi^2 EA + \tau^2 \frac{GA}{\beta_b} \right) T_{k-1}(\xi_i) \right\} - \sum_{k=1}^{K+2} c_k \frac{2\tau}{S} \left(\frac{GA}{\beta_n} + \frac{GA}{\beta_b} \right) T'_{k-1}(\xi_i) - \sum_{k=1}^{K+2} e_k \tau \frac{GA}{\beta_b} T_{k-1}(\xi_i) - \sum_{k=1}^{K+2} f_k \frac{2}{S} \frac{GA}{\beta_n} T'_{k-1}(\xi_i) = -\omega^2 \rho A \sum_{k=1}^{K+2} b_k T_{k-1}(\xi_i), \tag{A.2}$$

$$\sum_{k=1}^{K+2} a_k \chi\tau \frac{GA}{\beta_n} T_{k-1}(\xi_i) + \sum_{k=1}^{K+2} b_k \frac{2\tau}{S} \left(\frac{GA}{\beta_n} + \frac{GA}{\beta_b} \right) T'_{k-1}(\xi_i) + \sum_{k=1}^{K+2} c_k \left\{ \frac{4}{S^2} \frac{GA}{\beta_b} T''_{k-1}(\xi_i) - \tau^2 \frac{GA}{\beta_n} T_{k-1}(\xi_i) \right\} + \sum_{k=1}^{K+2} e_k \frac{2}{S} \frac{GA}{\beta_b} T'_{k-1}(\xi_i) - \sum_{k=1}^{K+2} f_k \tau \frac{GA}{\beta_n} T_{k-1}(\xi_i) = -\omega^2 \rho A \sum_{k=1}^{K+2} c_k T_{k-1}(\xi_i), \tag{A.3}$$

$$\sum_{k=1}^{K+2} d_k \left\{ \frac{4GJ}{S^2} T''_{k-1}(\xi_i) - \chi^2 EI_n T_{k-1}(\xi_i) \right\} - \sum_{k=1}^{K+2} e_k \frac{2\chi}{S} (EI_n + GJ) T'_{k-1}(\xi_i) + \sum_{k=1}^{K+2} f_k \chi\tau EI_n T_{k-1}(\xi_i) = -\omega^2 \rho J \sum_{k=1}^{K+2} d_k T_{k-1}(\xi_i), \tag{A.4}$$

$$-\sum_{k=1}^{K+2} b_k \tau \frac{GA}{\beta_b} T_{k-1}(\xi_i) - \sum_{k=1}^{K+2} c_k \frac{2}{S} \frac{GA}{\beta_b} T'_{k-1}(\xi_i) + \sum_{k=1}^{K+2} d_k \frac{2\chi}{S} (EI_n + GJ) T'_{k-1}(\xi_i) + \sum_{k=1}^{K+2} e_k \left\{ \frac{4}{S^2} EI_n T''_{k-1}(\xi_i) - \left(\frac{GA}{\beta_b} + \chi^2 GJ + \tau^2 EI_b \right) T_{k-1}(\xi_i) \right\} - \sum_{k=1}^{K+2} f_k \frac{2\tau}{S} (EI_n + EI_b) T'_{k-1}(\xi_i) = -\omega^2 \rho I_n \sum_{k=1}^{K+2} e_k T_{k-1}(\xi_i), \tag{A.5}$$

$$\sum_{k=1}^{K+2} a_k \chi \frac{GA}{\beta_n} T_{k-1}(\xi_i) + \sum_{k=1}^{K+2} b_k \frac{2}{S} \frac{GA}{\beta_n} T'_{k-1}(\xi_i) - \sum_{k=1}^{K+2} c_k \tau \frac{GA}{\beta_n} T_{k-1}(\xi_i)$$
$$+ \sum_{k=1}^{K+2} d_k \tau \chi EI_n T_{k-1}(\xi_i) + \sum_{k=1}^{K+2} e_k \frac{2\tau}{S} (EI_n + EI_b) T'_{k-1}(\xi_i)$$
$$+ \sum_{k=1}^{K+2} f_k \left\{ \frac{4}{S^2} EI_b T''_{k-1}(\xi_i) - \left(\frac{GA}{\beta_n} + \tau^2 EI_n \right) T_{k-1}(\xi_i) \right\} = -\omega^2 \rho I_b \sum_{k=1}^{K+2} f_k T_{k-1}(\xi_i),$$
$$(i = 1, \ldots, K) \tag{A.6}$$

The notation $'$ stands for the differentiations with respect to ξ.

Appendix B. Boundary conditions as series expansions at $\xi_b = \pm 1$

$$Fixed: \quad \begin{cases} \sum_{k=1}^{K+2} a_k T_{k-1}(\xi_b) = 0, & \sum_{k=1}^{K+2} b_k T_{k-1}(\xi_b) = 0, & \sum_{k=1}^{K+2} c_k T_{k-1}(\xi_b) = 0, \\ \sum_{k=1}^{K+2} d_k T_{k-1}(\xi_b) = 0, & \sum_{k=1}^{K+2} e_k T_{k-1}(\xi_b) = 0, & \sum_{k=1}^{K+2} f_k T_{k-1}(\xi_b) = 0, \end{cases} \tag{B.1}$$

$$Hinged: \quad \begin{cases} \sum_{k=1}^{K+2} a_k T_{k-1}(\xi_b) = 0, & \sum_{k=1}^{K+2} b_k T_{k-1}(\xi_b) = 0, & \sum_{k=1}^{K+2} c_k T_{k-1}(\xi_b) = 0, \\ \sum_{k=1}^{K+2} \left\{ d_k \frac{2}{S} T'_{k-1}(\xi_b) - e_k \chi T_{k-1}(\xi_b) \right\} = 0 \\ \sum_{k=1}^{K+2} \left\{ (d_k \chi - f_k) T_{k-1}(\xi_b) + e_k \frac{2}{S} T'_{k-1}(\xi_b) \right\} = 0, \\ \sum_{k=1}^{K+2} \left\{ e_k \tau T_{k-1}(\xi_b) + f_k \frac{2}{S} T'_{k-1}(\xi_b) \right\} = 0, \end{cases} \tag{B.2}$$

$$Free: \quad \begin{cases} \sum_{k=1}^{K+2} \left\{ a_k \frac{2}{S} T'_{k-1}(\xi_b) - b_k \chi T_{k-1}(\xi_b) \right\} = 0, \\ \sum_{k=1}^{K+2} \left\{ (a_k \chi - c_k \tau - f_k) T_{k-1}(\xi_b) + b_k \frac{2}{S} T'_{k-1}(\xi_b) \right\} = 0, \\ \sum_{k=1}^{K+2} \left\{ (b_k \tau + e_k) T_{k-1}(\xi_b) + c_k \frac{2}{S} T'_{k-1}(\xi_b) \right\} = 0, \\ \sum_{k=1}^{K+2} \left\{ d_k \frac{2}{S} T'_{k-1}(\xi_b) - e_k \chi T_{k-1}(\xi_b) \right\} = 0, \\ \sum_{k=1}^{K+2} \left\{ (d_k \chi - f_k \tau) T_{k-1}(\xi_b) + e_k \frac{2}{S} T'_{k-1}(\xi_b) \right\} = 0, \\ \sum_{k=1}^{K+2} \left\{ e_k \tau T_{k-1}(\xi_b) + f_k \frac{2}{S} T'_{k-1}(\xi_b) \right\} = 0. \end{cases} \tag{B.3}$$

The notation $'$ stands for the differentiations with respect to ξ.

References

[1] W.H. Wittrick, On elastic wave propagation in helical springs, *International Journal of Mechanical Sciences* 8 (1966) 25–47.
[2] D. Pearson, The transfer matrix method for the vibration of compressed helical springs, *Journal of Mechanical Engineering Science* 24 (1982) 163–171.
[3] K. Nagaya, S. Takeda, Y. Nakata, Free vibration of coil springs of arbitrary shape, *International Journal for Numerical Methods in Engineering* 23 (1986) 1081–1099.
[4] V. Yildirim, Investigation of parameters affecting free vibration frequencies of helical springs, *International Journal for Numerical Methods in Engineering* 39 (1996) 99–114.
[5] V. Yildirim, Free vibration analysis of non-cylindrical coil springs by combined used of the transfer matrix and the complementary functions method, *Communications in Numerical Methods in Engineering* 13 (1997) 487–494.
[6] V. Yildirim, Expression for predicting fundamental natural frequencies of non-cylindrical helical springs, *Journal of Sound and Vibration* 252 (2002) 479–491.
[7] L.E. Becker, G.G. Chassie, W.L. Cleghorn, On the natural frequencies of helical compression springs, *International Journal of Mechanical Sciences* 44 (2002) 825–841.
[8] J. Lee, D.J. Thompson, Dynamic stiffness formulation, free vibration and wave motion of helical springs, *Journal of Sound and Vibration* 239 (2001) 297–320.
[9] J.E. Mottershead, Finite elements for dynamical analysis of helical rods, *International Journal of Mechanical Sciences* 22 (1980) 267–283.
[10] Y. Xiong, B. Tabarrok, A finite element model for the vibration of spatial rods under various applied loads, *International Journal of Mechanical Sciences* 34 (1992) 41–51.
[11] N. Stander, R.J. Du Preez, Vibration analysis of coil springs by means of isoparametric curved beam finite elements, *Communications in Applied Numerical Methods* 8 (1992) 373–383.
[12] J.P. Boyd, *Chebyshev & Fourier Spectral Methods, Lecture Notes in Engineering 49*, Springer, New York, 1989.
[13] J. Lee, W.W. Schultz, Eigenvalue analysis of Timoshenko beams and axisymmetric Mindlin plates by the pseudospectral method, *Journal of Sound and Vibration* 269 (2004) 609–621.
[14] J. Lee, Eigenvalue analysis of double-span Timoshenko beams by pseudospectral method, *Journal of Mechanical Science and Technology* 19 (2005) 1753–1760.